JOURNAL OF CATALYSIS 112, 444–452 (1988)

Temperature-Programmed Desorption Study of Ammonia Desorption–Diffusion in Molecular Sieves

II. Application to Partially Decationated Y-Zeolites

LUCIO FORNI,*,[1] ENRICO MAGNI,* EMANUELE ORTOLEVA,* ROBERTO MONACI,† AND VINCENZO SOLINAS†

*Dipartimento di Chimica Fisica ed Elettrochimica, Università di Milano, Via C. Golgi 19, 20133 Milano, Italy, and †Dipartimento di Scienze Chimiche, Università di Cagliari, Via Ospedale 72, 09100 Cagliari, Italy

Received September 18, 1987; revised February 18, 1988

An analysis of TPD data relating to the desorption of ammonia from two different samples of partially decationated Y-zeolite is reported, assuming various chemical or physical steps to be rate-determining. The process is shown to be controlled by intracrystalline surface diffusion, with values of the apparent activation energy E_a = 30.8 and 27.1 kcal/mol, respectively, for the two zeolite samples. These values include the retardation effect associated with the hindering interaction of the diffusing ammonia molecules with the acid sites of the zeolite. Values of the apparent effective diffusion coefficient ranging from ca. 3 10^{-18} to ca. 4 10^{-14} cm^2/s have been calculated for the 423–573 K temperature range.

INTRODUCTION

Zeolites are among the most important solid acid catalysts. They are extensively employed in many large-scale industrial processes involving molecular transformation of hydrocarbons, such as reforming, isomerization, alkylation and disproportionation (*1–4*). The activity of these catalysts is due to the presence of surface acid centers of Brønsted and/or Lewis type and many methods have been proposed and commonly employed for determining their strength and concentration (*5–11*).

In Part I (*12*) of the present work, the theory of the TPD technique and its application to the use of ammonia for the characterization of acid zeolites has been extensively discussed. The equations describing the TPD process have been derived for the most important cases, i.e., when desorption of the base (with no readsorption or with free readsorption of the latter) or diffusion of the desorbed ammonia within the zeolite pores is the controlling step. In this paper (Part II) we report on the application of such equations to the study of ammonia TPD from two differently decationated Y-zeolites, previously employed as effective and selective catalysts for the alkylation of thiophene with methanol (*13*) and for the isomerization of 1-methylnaphthalene to 2-methylnaphthalene (*14*), respectively.

EXPERIMENTAL

Materials. Ultrapure (≥99.9999 vol%) He was used as carrier gas. It was further purified by passing through a glass trap, cooled in liquid N_2, and filled with 13X zeolite particles (60–80 mesh), frequently regenerated by calcination overnight at 823 K in a slow flow of dry air (≥99.999 vol% pure). Gaseous ammonia, ≥99.9995 vol% pure, was used as supplied.

Zeolite. The partially decationated zeolite was prepared from Union Carbide LZY-52 powder cake, by ion exchange with NH_4Cl solution, followed by drying and calcination at 823 K in slowly flowing dry air. Analysis by atomic absorption spectrome-

[1] To whom correspondence should be addressed.

0021-9517/88 $3.00

try showed that ca. 30 or ca. 55%, respectively, of the original Na^+ content had been exchanged by H^+, the following being the chemical composition (wt%) of the final solid: Na_2O 9.35, Al_2O_3 23.5, SiO_2 65.5, and 6.10, 24.1, 67.1, respectively, for the two samples, denoted HNaY-30 and HNaY-55. XRD analysis (Debye method, Cu$K\alpha$ radiation, Ni-filtered) of both samples, before and after the complete series of TPD experiments, showed a pattern identical with that of the original, unexchanged zeolite. The dimensions of the zeolitic microcrystals, measured on several micrographs obtained by SEM, were of the order of 1 μm.

Apparatus and procedure. A conventional TPD apparatus was employed, equipped with a quartz microreactor (1 cm i.d.) and a Philips Thermocoax miniature thermocouple, inserted in a 0.25-mm-o.d. Inconel sheath. A sketch is given in Fig. 1. Both the signals, that from the thermocouple embedded in the zeolite particles and that from the thermal conductivity (TC) detector, were sent to a multichannel AD converter and the data were collected, preliminarily processed, and stored on minicassette by a small Epson HX20 computer. Further processing was made after transferring the data to a Gould SEL 32/90 computer.

Before the experiment, the zeolite sample (50–100 mg) was purged by heating overnight at 823 K in a slow flow (1–2 cm^3/min) of dry air and then kept at the same temperature for 24 h in a similar flow of He. To keep the zeolite clean between successive TPD runs, it was continuously maintained at 823 K in slowly flowing He.

All the TPD runs were carried out with a He flow rate of 30 cm^3/min and by increasing the temperature at a rate $\beta = 10$ K/min. These conditions were chosen after a series of preliminary experiments as the best compromise, allowing perfect reproducibility of the experimental data (*15*). Presaturation of the sample was made using the gas sampling valve by injecting a sufficient number of pulses of gaseous ammonia into the He

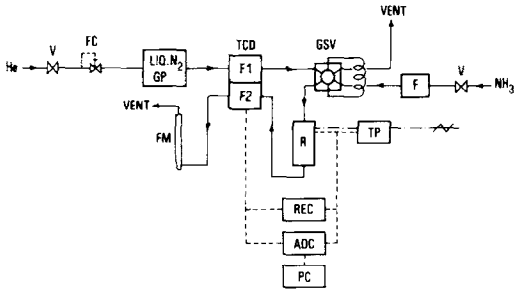

FIG. 1. Sketch of the TPD apparatus. V, shut-off valve; FC, flow controller; GP, gas purifier; TCD, thermal conductivity detector; F1, F2, hot filaments; GSV, gas sampling valve; R, reactor; FM, soap-bubble flow meter; TP, temperature programmer; REC, multipen strip-chart recorder; ADC, analog-to-digital converter; PC, computer.

carrier (5 cm^3/min) before the sample, kept at the chosen starting temperature T_0 of the actual TPD run. The zeolite was then left at T_0 under a He flow rate of 30 cm^3/min until the physically adsorbed base was completely removed. This isothermal desorption time t_{id} was determined for each value of T_0 through a series of experiments by progressively increasing t_{id} until the amount of NH_3 desorbed during a subsequent TPD run did not change further. The signal of the TC detector was always corrected by subtracting point by point the signal collected by a corresponding blank run carried out under the same conditions, but in the absence of zeolite.

RESULTS

In the present work, the lower temperature limit of the TPD runs was set at 423 and 448 K for HNaY-30 and HNaY-55, respectively. The upper limit was set at 823 K for both samples. This was done by considering that under the usual working conditions of the zeolite as a catalyst, all the very weak sites remain free, while the strongest ones are permanently occupied. As a consequence, only the medium-strength sites are involved in the catalytic reaction. Another reason for the upper temperature

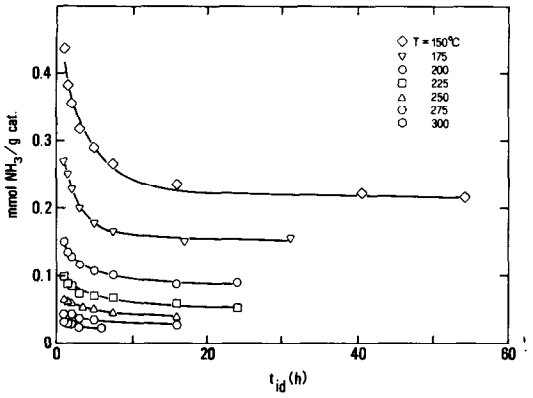

FIG. 2. Experimental determination of the isothermal desorption time, t_{id}, at varying temperatures. HNaY-30 zeolite.

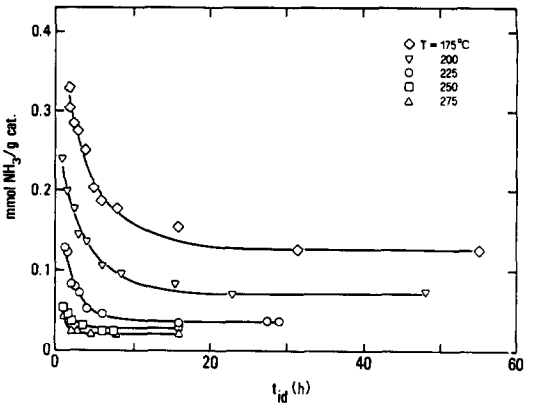

FIG. 3. As Fig. 2, but for HNaY-55 zeolite.

limit is that Y-zeolite tends to lose some water irreversibly at temperatures in excess of 843 K, with a progressive modification of the original framework structure (*16*). As a consequence, we define as $\theta = 1$ and $\theta = 0$ the surface coverage at 423 (or 448) and 823 K, respectively. Thus, $\theta = 1$ does not correspond to the overall number of acid sites present on our sample, but it refers to the sites permanently occupied by ammonia at 423 (or 448) K, minus the sites permanently occupied at 823 K. Similarly, $\theta = 0$ refers to the fact that the sites remaining occupied at $T > 823$ K are not considered. Hence, $\theta(T)$ is the coverage at temperature T, referred to $\theta(423, \text{ or } 448) = 1$ and $\theta(823) = 0$.

Amount of undesorbed base at varying temperatures. The data for the determination of the ammonia chemically held at different temperatures, collected as mentioned, are shown in Figs. 2 and 3, for the two zeolite samples, respectively. It can be seen immediately that the lower the temperature, the longer is the isothermal desorption time t_{id}. The latter may easily reach many hours, up to almost 2 days for $T = 423$ K and more than 1 day for $T = 448$ K. As a consequence, the amount N_∞ of ammonia chemically adsorbed at different temperatures was determined by carrying out a series of TPD runs with different starting temperatures, 25 K apart, after the proper t_{id} had passed. The results are collected in Table 1.

Experimental TPD data. The experimental TPD curves, collected for each zeolite, are shown in Figs. 4 and 5, respectively. In Figs. 6 and 7, the difference peaks are shown, these being obtained by subtracting point by point the values of the $(T_{0i} + \Delta T)$ curve from those of the T_{0i} curve of Figs. 4 and 5, respectively.

ANALYSIS OF DATA

Evaluation of the $N_\infty(T)$ function. Five different simple interpolating functions were tried for the purpose of correlating the experimental data of Table 1 and searching

TABLE 1

Amount of Ammonia Chemically Held as a Function of Temperature (Experimental Data)

T (K)	N_∞ (mmol/g zeolite)	
	HNaY-30	HNaY-55
423	0.195	—
448	0.106	0.145
473	0.051	0.091
498	0.034	0.055
523	0.021	0.037
548	0.013	0.026
573	0.008	—

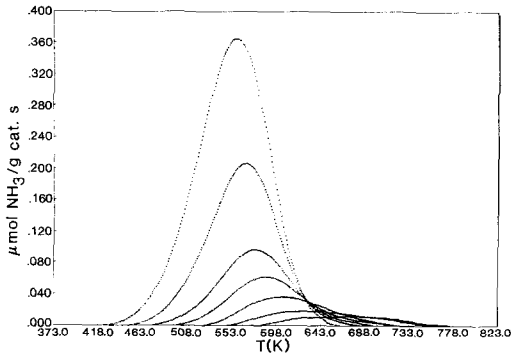

FIG. 4. Experimental TPD curves (1 K steps) for HNaY-30. Linear temperature increase: 10 K/min, He flow rate F = 30 cm³/min. Values corrected by subtracting the corresponding blank run data (see text).

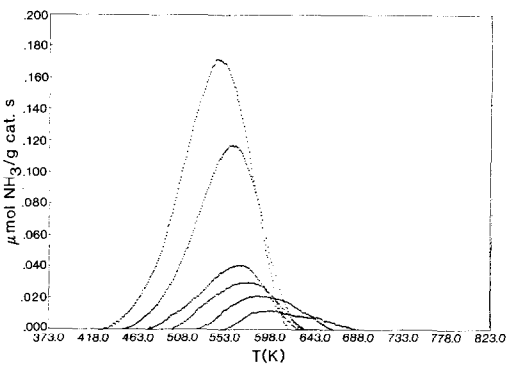

FIG. 6. Experimental difference peaks for HNaY-30 zeolite.

for the form of the function $N_\infty = N_\infty(T)$: these were four polynomials of increasing order (from the parabola up to the fifth-order equation) and the simple exponential

$$N_\infty = \exp(A_1 + A_2/T). \quad (1)$$

The latter gave the best result and the values of the parameters A_1 and A_2, determined by the least-squares procedure, are collected in Table 2.

Equations employed. The equations derived in Part I (*12*) for the determination of kinetic or thermodynamic parameters are the following.

(i) If desorption of ammonia is controlling and readsorption of the desorbed base does not occur significantly,

$$\Delta q \ln(\Delta q/\Delta q_0) \frac{1}{d(\Delta q)/dT} = \exp(E_d/RT)I \quad (2)$$

$$I = \int_{T_0}^{T} \exp(-E_d/RT)dT \quad (3)$$

$$A = -\exp(E_d/RT) \frac{1}{\Delta q} \frac{d(\Delta q)}{dt}. \quad (4)$$

(ii) For the same situation, a much simpler and safer approach (*12*) is based on the equation

$$-d(\Delta q)/dt = A\ \Delta q \exp(-E_d/RT). \quad (5)$$

(iii) When readsorption of the base occurs freely,

$$\Delta q_0 \ln(\Delta q/\Delta q_0) + \Delta q_0 - \Delta q = ((\Delta q_0 - \Delta q)/\Delta q)(d(\Delta q)/dt) \times \exp(\Delta H_d/RT)I' \quad (6)$$

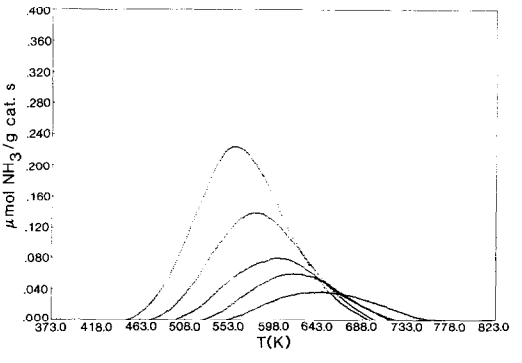

FIG. 5. As Fig. 4, but for HNaY-55.

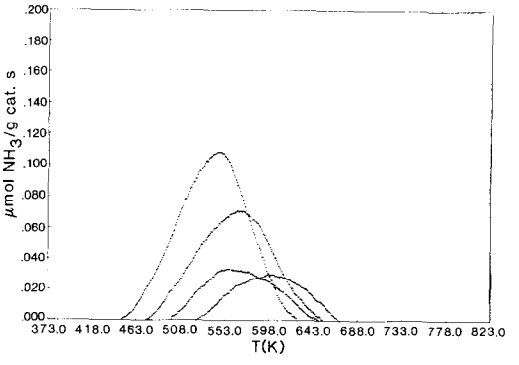

FIG. 7. Experimental difference peaks for HNaY-55 zeolite.

TABLE 2

Parameters of the Function $N_\infty = \exp(A_1 + A_2/T)$, as Determined by the Least-Squares Procedure

Zeolite	A_1	A_2	Correl. coeff.
HNaY-30	−13.6 ± 0.2	5059. ± 107.	0.9989
HNaY-55	−11.5 ± 0.1	4273. ± 73.	0.9996

$$I' = \int_{T_0}^{T} \exp(-\Delta H_d/RT)dT. \quad (7)$$

(iv) Finally, the equation

$$-dN/dt = M_{\Delta t}/\Delta t, \quad (8)$$

where

$$M_{\Delta t_i} = (N(T_i) - N_\infty(T_i^*))(1 - (6/\pi^2) \sum_{n=1}^{\infty} (1/n^2) \exp(-(D_e/R_c^2)(T_i^*)n^2\pi^2\Delta t_i)) \quad (9)$$

in which

$$\begin{aligned} N(T_1) &= N_\infty(T_1) && (i = 1) \\ N(T_i) &= N(T_{i-1}) + M_{\Delta t_{i-1}} && (i > 1) \end{aligned} \quad (10)$$

must be employed if intracrystalline diffusion of the base within the zeolite pores is rate-controlling.

In Eqs. (2)–(6), Δq (mmol/g of solid) represents the amount of ammonia held by energetically homogeneous acid centers at temperature T and Δq_0 is Δq at temperature T_0; A and E_d are the preexponential factor and the apparent activation energy for the process of ammonia desorption from such centers. In Eqs. (6) and (7), ΔH_d is the enthalpy change associated with the desorption process. In Eq. (9), $M_{\Delta t_i}$ (mmol/g of solid) represents the amount of ammonia coming out of the zeolite during the time interval Δt_i, R_c (cm) is the radius of the zeolite crystals, assumed spherical, $D_e(T_i)$, (cm^2/s) is the apparent effective diffusion coefficient, $N(T_i)$ is the amount of ammonia still present in the solid at $T = T_i$, and $N_\infty(T_i^*)$ is the amount of ammonia that will not leave the solid at $T = T_i^* = (T_{i-1} + 0.5)$ K, i.e., the ammonia chemically held by the zeolite at such a temperature.

Desorption controlling with no readsorption. A first analysis was carried out on the basis of Eqs. (2)–(4) and of the data of Figs. 6 and 7. Following this procedure, the value of E_d was first optimized by nonlinear regression on Eqs. (2) and (3) and then A was evaluated by averaging the values calculated point by point through Eq. (4). The results obtained in this way are shown in Table 3, columns 3 and 4. The integral I (Eq. (3)) has been calculated numerically by inserting a subroutine based on Simpson's rule in the main nonlinear regression program. As described in detail in Part I (*12*), three improvements have thereby been made with respect to the original procedure (*11*). The first is the mentioned numerical solution of the analytically unsolvable integral I, with respect to the graphical solution proposed there. The second is that the difference ΔT between the initial temperatures T_0 of two successive TPD curves has been halved, by putting $\Delta T = 25$ K (instead of 50 K), so to consider as much more homogeneous the energy of the sites characterized by a given pair of E_d and A values. The third is that the values of E_d and A are obtained by making use of the whole set of the experimental data describing the TPD peak, instead of referring only to the peak maximum.

However, this procedure is based on the direct optimization of only one kinetic parameter (E_d). The other (A) is calculated out of the optimization routine, so that, when drawing the calculated difference peak, by employing the values of E_d and A so obtained, a poor fit was noted in most cases (see, e.g., Fig. 8).

A much better fit was obtained by employing our modified procedure (*12*), in which the simultaneous optimization of both kinetic parameters, by nonlinear regression, is based on Eq. (5). A typical example is shown in Fig. 9, referring to the same difference curve of Fig. 8. The optimized values of the parameters, as obtained

TABLE 3

Optimized Kinetic Parameters of Eqs. (2)–(5)

T_0 (K)	$T_0 + \Delta T$ (K)	E_d (kcal/mol) (through Eqs. (2)–(4))	A (s^{-1}) (through Eqs. (2)–(4))	E_d (kcal/mol) (through Eq. (5))	A (s^{-1}) (through Eq. (5))
			HNaY-30		
423	448	21.0	1.33E + 06	16.9	2.65E + 04
448	473	22.4	3.04E + 06	18.5	8.07E + 04
473	498	23.7	9.36E + 06	19.8	2.30E + 05
498	523	26.0	5.00E + 07	20.7	3.76E + 05
523	548	25.0	7.90E + 06	19.9	8.71E + 04
548	573	23.2	9.21E + 05	18.4	1.52E + 04
			HNaY-55		
448	473	18.5	1.19E + 05	15.3	5.67E + 03
473	498	18.8	7.49E + 04	15.6	3.88E + 03
498	523	20.4	2.90E + 05	16.0	5.03E + 03
523	548	24.8	5.69E + 06	19.1	3.55E + 04

through this modified procedure, are collected in Table 3, columns 5 and 6.

Desorption controlling with free readsorption. If the desorbed base can readsorb freely, Eqs. (6) and (7) may be employed for the evaluation of ΔH_d. The procedure followed here was to analyze each difference peak in several points. The evaluation of the integral I' was carried out numerically, as for I, by Simpson's rule.

Similar results were obtained with this procedure for the whole set of difference peaks of both zeolites. A typical example is shown in Table 4.

Intracrystalline diffusion controlling. In this case, Eqs. (8)–(10) are employed for the direct analysis of the primary TPD data (curves of Figs. 4 and 5). Of course, the apparent effective diffusion coefficient, appearing in Eq. (9), in addition to the physical restriction due to the narrowness of zeolitic pores, must also take into account

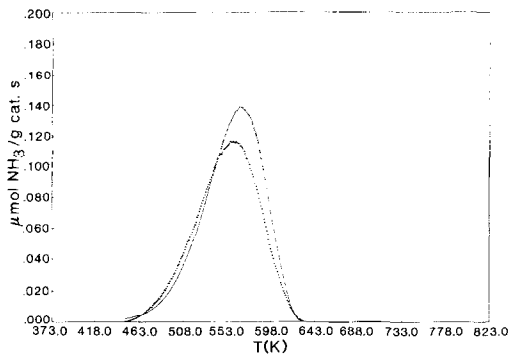

FIG. 8. Typical example of poor fit between the experimental difference peak and the corresponding curve, calculated through Eqs. (2)–(4) and the optimized parameters of Table 3, columns 3 and 4. T_0 = 448 K, $T_0 + \Delta T$ = 473 K, HNaY-30 zeolite.

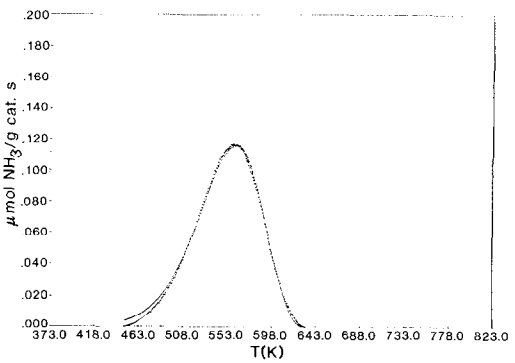

FIG. 9. Typical fit between experimental difference peak and the corresponding curve, calculated through Eq. (5) and the optimized parameters of Table 3, columns 5 and 6. T_0 = 448 K, $T_0 + \Delta T$ = 473 K, HNaY-30 zeolite.

TABLE 4

Typical Results Obtained When Assuming Desorption Controlling with Free Readsorption (Eqs. (6) and (7))

Point (T (K)) considered	ΔH_d (kcal/mol)
448	94.8
473	57.0
498	45.3
523	37.4
544[a]	33.1
548	31.8
573	26.4
598	24.9

Note. Zeolite HNaY-30. T_0 = 423 K; $T_0 + \Delta T$ = 448 K.

[a] Peak maximum.

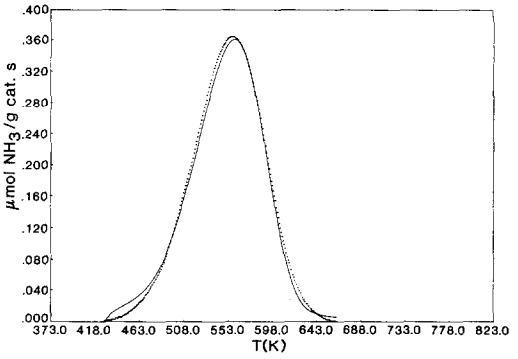

FIG. 10. Typical fit between experimental TPD data and the corresponding curve, calculated through Eqs. (9) and (10) (together with Eqs. (1) and (11)) and the optimized parameters of Tables 2 and 5. T_0 = 448 K, HNaY-55 zeolite.

the additional slowing phenomena connected with the interaction of the base with the surface acid sites which are covering the pore walls of the zeolite.

The best function expressing the dependence of (D_e/R_c^2) on temperature was found to be of the form proposed elsewhere (*17*):

$$D_e/R_c^2 = A_a \exp(-E_a/T). \qquad (11)$$

A subroutine for the solution of Eq. (11) was then inserted in the nonlinear regression–optimization routine based on Eq. (9). As for the values of N_∞ at the varying temperatures, Eq. (1) was employed, together with the optimized parameters A_1 and A_2, collected in Table 2.

The values of kinetic parameters E_a and A_a, obtained from the analysis of the whole set of our TPD curves, are collected in Table 5. A typical example of the fit between the experimental data and the calculated curve is shown in Fig. 10.

DISCUSSION

The results of the present analysis may be discussed on the basis of a comparison between what is expected from the calculation, based on every mechanism assumed, and what has been actually obtained.

Equations (2)–(4) or, better, Eq. (5), referring to desorption controlling with no readsorption, must lead to different values of the kinetic parameters E_d and A, when applied to the various difference peaks, relative to the same zeolite and obtained by increasing progressively the starting temperature T_0 of the TPD run. Indeed, by increasing the latter parameter, only stronger and stronger sites may still hold the base, the weaker ones becoming progressively

TABLE 5

Optimized Kinetic Parameters of Eq. (11)

T_0 (K)	E_a (kcal/mol)	A_a (s^{-1})
	HNaY-30	
423	32.6	1.80E + 01
448	36.2	2.09E + 01
473	31.4	1.60E + 01
498	33.2	1.73E + 01
523	31.6	1.52E + 01
548	22.8	6.62E + 00
573	27.7	9.49E + 00
	HNaY-55	
448	24.4	1.01E + 01
473	26.4	1.12E + 01
498	24.3	8.76E + 00
523	31.7	1.46E + 01
548	28.6	1.10E + 01

free. As a consequence, higher and higher values of E_d are expected, with increasing T_0.

When assuming free readsorption (Eqs. (6) and (7), provided the temperature difference ΔT between the starting temperature T_0 of two TPD curves (whose difference gave the actual difference peak) is sufficiently small, one expects the same value of ΔH_d for the whole set of points forming a given difference peak. Indeed, a small ΔT corresponds to a given group of energetically homogenous sites, with which a common value of the desorption enthalpy change is associated.

Finally, the last mechanism considered, namely that assuming intracrystalline diffusion to be controlling, is the only one referring to a physical rather than to a chemical phenomenon as the rate-determining step of the overall process. In this case, a common value of the apparent kinetic parameters E_a and A_a is expected for the whole set of TPD curves, referring to the same zeolite, the diffusion process being practically independent of the strength of surface acid sites.

The data of Tables 3 and 4 point to exclusion of both desorption-controlled mechanisms as rate-determining. Indeed, in the first case (Table 3), the values of E_d and A are practically constant for each zeolite. In the second case (Table 4), the values of ΔH_d decrease monotonically with increasing temperature of the point considered along the difference peak curve. No casual distribution of the data around a common average value was ever observed for any of our difference peaks. As a consequence, both models for which Eqs. (2)–(7) were derived must be discarded as incapable of representing the phenomena analyzed.

Our data are certainly much better interpreted assuming the intracrystalline diffusion (Eq. (9)) to be the controlling step. Indeed, the data of Table 5 show that a common, average value of $E_a = 30.8 \pm 4.0$ and 27.1 ± 2.8 kcal/mol can be calculated for HNaY-30 and HNaY-55 zeolites, respectively, and no particular trend of the E_a values can be noted with increasing T_0. The corresponding average values of A_a are 14.8 ± 4.6 and 11.1 ± 1.9 s^{-1}, respectively. By inserting these average values of E_a and A_a in Eq. (11) and assuming $R_c \simeq 10^{-4}$ cm, values of the apparent effective diffusion coefficient D_e (cm^2/s) ranging from 2.9×10^{-18} to 4.3×10^{-14} for HNaY-30 and from 5.9×10^{-18} to 2.8×10^{-14} for HNaY-55 can be calculated for the 423–573 K temperature range.

These results show that, as expected, the higher the temperature the easier is the diffusion of ammonia molecules through the zeolite channels. Furthermore, the presence of the mentioned retardation effect on surface diffusion (associated with the hindering interaction of the diffusing basic molecules with the acid sites of the solid) is confirmed by the low values of D_e obtained and by the high values of t_{id} required for good reproducibility of the experimental data.

REFERENCES

1. Venuto, P. B., *in* "Catalysis in Organic Synthesis" (G. V. Smith, Ed.), p. 67. Academic Press, New York, 1977.
2. Flanigen, E. M., *Pure Appl. Chem.* **52,** 2191 (1980).
3. Haag, W. O., "Proc. VI Intern. Zeolite Conf., Reno, Nevada, July 1983" (D. H. Olson and A. Bisio Eds.), p. 466. Butterworths, Tonbridge, England.
4. Hölderich, W., *in* "New Developments in Zeolite Science and Technology" (Y. Murakami, A. Iijima, and J. W. Ward, Eds.), p. 827. Kodansha-Elsevier, Tokyo, 1986.
5. Atkinson, D., and Curthoys, G., *Chem. Soc. Rev.* **8,** 475 (1979).
6. Bezman, R., *J. Catal.* **68,** 242 (1981).
7. Jacobs, P. A., *Catal. Rev. Sci. Eng.* **24,** 415 (1982).
8. Skeels, G. W., and Flank, W. H., *in* "Intrazeolite Chemistry" (G. D. Stucky and F. D. Dwyer, Eds.), ACS Symp. Ser. Vol., 218, p. 369. 1983.
9. Rhee, K. H., Brown, F. R., Finseth, D. H., and Stencel, J. M., *Zeolites* **3,** 344 (1983).
10. Karge, H. G., Sarbak, Z., Hatada, K., Weitkamp, J., and Jacobs, P. A., *J. Catal.* **82,** 236 (1983).

11. Hashimoto, K., Masuda, T., and Mori, T., *in* "New Developments in Zeolite Science and Technology" (Y. Murakami, A. Iijima, and J. W. Ward, Eds.), p. 503. Kodansha-Elsevier, Tokyo, 1986.

12. Forni, L., and Magni, E., *J. Catal.* **112,** 437 (1988).

13. Solinas, V., Monaci, R., Marongiu, B., and Forni, L., *Acta Phys. Chem. Szeged. Nova Ser.* **31**(1–2), 291 (1985).

14. Solinas, V., Monaci, R., Marongiu, B., and Forni, L., *Appl. Catal.* **9,** 109 (1984).

15. Lemaitre, J. L., *in* "Characterization of Heterogeneous Catalysts" (F. Delannay, Ed.), p. 29. Dekker, New York, 1984.

16. Breck, D. W., "Zeolite Molecular Sieves." Wiley, New York, 1974.

17. Satterfield, C. N., "Mass Transfer in Heterogeneous Catalysis." MIT Press, Cambridge, MA 1970.